

- [18] M. Huber and R. A. Gruben, "2-D contact detection and localization using proprioceptive information," *IEEE Trans. Robot. Autom.*, vol. 10, no. 1, pp. 23–33, Feb. 1994.
- [19] K. Gunnarsson and F. Prinz, "CAD model-based localization of parts in manufacturing," *Comput.*, vol. 20, pp. 66–74, Aug. 1987.
- [20] S. Haidacher and G. Hirzinger, "Contact point identification in multi-fingered grasps exploiting kinematic constraints," in *Proc. IEEE Int. Conf. Robotics Automation*, 2002, pp. 1597–1603.
- [21] R. D. Howe and M. R. Cutkosky, "Dynamic tactile sensing: Perception of fine surface features with stress rate sensing," *IEEE Trans. Robot. Autom.*, vol. 9, no. 2, pp. 140–151, Apr. 1993.
- [22] R. D. Howe *et al.*, "Grasping, manipulation, and control with tactile sensing," in *Proc. IEEE Int. Conf. Robotics Automation*, 1990, pp. 1258–1263.
- [23] Y.-B. Jia, "Grasping curved objects through rolling," in *Proc. IEEE Int. Conf. Robotics Automation*, 2000, pp. 377–382.
- [24] —, "Localization on curved objects using tactile information," in *Proc. IEEE/RSJ Int. Conf. Intell. Robots Syst.*, 2001, pp. 701–706.
- [25] —, "Contact sensing for parts localization: Sensor design and experiments," in *Proc. IEEE/RSJ Int. Conf. Intell. Robots Syst.*, 2003, pp. 516–522.
- [26] —, (2003) Tactile localization and reconstruction of curved objects. [Online]. Available: <http://www.cs.iastate.edu/~jia/papers/localize.pdf>
- [27] Y.-B. Jia and M. Erdmann, "Geometric sensing of known planar shapes," *Int. J. Robot. Res.*, vol. 15, pp. 365–392, Aug. 1996.
- [28] M. Kaneko and K. Tanie, "Contact point detection for grasping an unknown object using self-posture changeability," *IEEE Trans. Robot. Automat.*, vol. 10, no. 3, pp. 355–367, Jun. 1994.
- [29] D. J. Kriegman and J. Ponce, "On recognizing and positioning curved 3-D objects from image contours," *IEEE Trans. Pattern Anal. Mach. Intell.*, vol. 12, no. 12, pp. 1127–1137, Dec. 1990.
- [30] Z. Li and J. Canny, "Motion of two rigid bodies with rolling constraint," *IEEE Trans. Robot. Autom.*, vol. 6, no. 1, pp. 62–72, Feb. 1990.
- [31] Z. Li, J. Gou, and Y. Chu, "Geometric algorithms for workpiece localization," *IEEE Trans. Robot. Autom.*, vol. 14, no. 6, pp. 864–878, Dec. 1998.
- [32] K. Lynch, H. Maekawa, and K. Tanie, "Manipulation and active sensing by pushing using tactile feedback," in *Proc. IEEE/RSJ Int. Conf. Intell. Robots Syst.*, 1992, pp. 416–421.
- [33] C.-H. Menq, H.-T. Yau, and G.-Y. Lai, "Automated precision measurement of surface profile in CAD-directed inspection," *IEEE Trans. Robot. Autom.*, vol. 8, no. 2, pp. 268–278, Apr. 1992.
- [34] M. Moll and M. A. Erdmann, "Reconstructing shape from motion using tactile sensors," in *Proc. IEEE/RSJ Int. Conf. Intell. Robots Syst.*, 2001, pp. 692–700.
- [35] D. J. Montana, "The kinematics of contact and grasp," *Int. J. Robot. Res.*, vol. 7, pp. 17–32, Jun. 1988.
- [36] E. Paljug, X. Yun, and V. Kumar, "Control of rolling contacts in multi-arm manipulation," *IEEE Trans. Robot. Autom.*, vol. 10, no. 4, pp. 441–452, Aug. 1994.
- [37] M. H. Raibert and J. J. Craig, "Hybrid position/force control of manipulators," *J. Dynamic Syst., Measurement, Contr., Trans. ASME*, vol. 102, pp. 126–133, 1981.
- [38] A. Rao and K. Goldberg, "Placing registration marks," *IEEE Trans. Ind. Electron.*, vol. 41, no. 1, pp. 51–59, Feb. 1994.
- [39] K. Salisbury, "Interpretation of contact geometries from force measurements," in *Robot. Res.*, M. Brady and R. Paul, Eds. Cambridge, MA: MIT Press, 1984, pp. 565–577.
- [40] S. Shekhar, O. Khatib, and M. Shimojo, "Object localization with multiple sensors," *Int. J. Robot. Res.*, vol. 7, pp. 34–44, Dec. 1988.
- [41] B. Shimano and B. Roth, "On force sensing information and its use in controlling manipulators," in *Proc. Int. Feder. Automatic Control*, 1977, pp. 119–126.
- [42] T. Tsujimura and T. Yabuta, "Object detection by tactile sensing method employing force/torque information," *IEEE Trans. Robot. Autom.*, vol. 5, no. 4, pp. 444–450, Aug. 1989.
- [43] R. M. Voyles, J. D. Morrow, and P. K. Khosla, "The shape from motion approach to rapid and precise force/torque sensor calibration," *J. Dynamic Syst., Measurement, Contr.*, vol. 119, pp. 229–235, Jun. 1997.
- [44] A. S. Wallack, J. F. Canny, and D. Manocha, "Object localization using crossbeam sensing," in *Proc. IEEE Int. Conf. Robotics Automation*, 1993, pp. 692–699.
- [45] X. Zhou, Q. Shi, and Z. Li, "Contact localization using force/torque measurements," in *Proc. IEEE Int. Conf. Robotics Automation*, 1996, pp. 1339–1344.

A Simulation/Experimental Study of the Noisy Behavior of the Time-Domain Passivity Controller

Jee-Hwan Ryu, Blake Hannaford, Dong-Soo Kwon, and Jong-Hwan Kim

Abstract—A noisy behavior of the time-domain passivity controller during the period of low velocity is analyzed. Main reasons of the noisy behavior are investigated through a simulation with a one-DOF haptic interface model. It is shown that the PO/PC is ineffective in dissipating the produced energy when the sign of the velocity, which is numerically calculated from the measured position, is suddenly changed, and when this velocity is zero. These cases happen during the period of low velocity due to the limited resolution of the position sensor. New methods, ignoring the produced energy from the velocity sign change, and holding the control force while the velocity is zero, are proposed for removing the noisy behavior. The feasibility of the developed methods is proved with both a simulation and a real experiment.

Index Terms—Haptic interface, noisy behavior, passivity controller, passivity observer, time-domain passivity.

I. INTRODUCTION

A haptic interface is a kinesthetic link between a human operator and a virtual environment (VE). One of the most significant problems in haptic interface design is to create a control system which simultaneously is stable (i.e., does not exhibit vibration or divergent behavior) and gives high fidelity under any operating conditions and for any virtual environment parameters. There are several mechanisms by which a virtual environment or other part of the system might exhibit active behavior. These include quantization [4], interactions between the discrete time system and the continuous time device/human operator [5], and delays due to numerical integration schemes [14].

Initial efforts to solve this problem introduced the "virtual coupling" between the virtual environment and the haptic device [1], [4], [22]. The virtual coupling parameters can be set empirically, but several previous research projects have sought out a theoretical design procedure using control theory. However, interesting virtual environments are always nonlinear and the dynamic properties of a human operator are always involved. These factors make it difficult to analyze haptic systems in terms of system models with known parameters and linear control theory. Anderson and Spong [2] and Neimeyer and Slotine [15] have used passivity ideas in the related area of stable control of force-feedback teleoperation with time delay. Colgate and Schenkel [5] have used it to derive fixed parameter virtual couplings (i.e., haptic interface controllers). The major problem with using passivity for design of haptic

Manuscript received September 22, 2004; revised January 21, 2005. This paper was recommended for publication by Associate Editor C. Melchiorri and Editor I. Walker upon evaluation of the reviewers' comments. This work was supported in part by a grant from BK21 School of Information Technology of KAIST, and ITRC-Intelligent Robot Research Center of KAIST.

J.-H. Ryu is with the School of Mechanical Engineering, Korea University of Technology and Education, Cheonan-city 330-708, Korea (e-mail: jhryu@kut.ac.kr).

B. Hannaford is with the Department of Electrical Engineering, University of Washington, Seattle, WA 98195-2500, USA (e-mail: blake@u.washington.edu).

D.-S. Kwon is with the Department of Mechanical Engineering, Korea Advanced Institute of Science and Technology, Taejeon 305-701, Korea (e-mail: kwonds@kaist.ac.kr).

J.-H. Kim is with the Department of Electrical Engineering and Computer Science, Korea Advanced Institute of Science and Technology, Taejeon 305-701, Korea (e-mail: johkim@rit.kaist.ac.kr).

Digital Object Identifier 10.1109/TRO.2005.847611

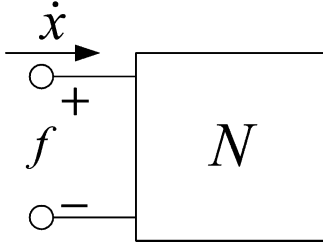


Fig. 1. One-port network.

interaction systems is that it is over conservative. In many cases performance can be poor if a fixed damping value is used to guarantee passivity under all operating conditions. Several other passivity based approaches were also proposed for stable haptic interaction [3], [10], [11].

A different passivity based approach has been proposed by Hannaford and Ryu [6], that measures active system behavior and injects variable damping whenever net energy is produced by the virtual environment. They proposed a “passivity observer” (PO) and a “passivity controller” (PC) to insure stable contact under a wide variety of operating conditions. Recently, the PO/PC approach has been improved for estimating exact energy output [17], and removing sudden impulsive PC force [18].

In our previous researches [6], [16]–[18], the PO/PC was ineffective in dissipating the produced energy during the period of low velocity (series type PC in impedance causality) or low force (parallel type PC in admittance causality), and it has been open as a future work. We have named this undesirable behavior as a “noisy behavior” due to the unwanted high frequency oscillations of position and force. Even though there has been an effort to solve the noise problem [8], it was a tuning method of heuristic control parameters depending on a system. In this paper, main reasons of the noisy behavior of the PO/PC are analyzed, and methods to remove the noisy behavior are proposed.

II. REVIEW OF THE TIME-DOMAIN PASSIVITY CONTROL

In this section, we briefly review time-domain passivity control. First, we define the sign convention for all forces and velocities so that their product is positive when power enters the system port (Fig. 1). Also, the system is assumed to have initial stored energy $E(0) = 0$ at $t = 0$. The following widely known definition of passivity is used.

Definition 1: The one-port network N with initial energy storage $E(0) = 0$ is *passive* if and only if

$$\int_0^t f(\tau)\dot{x}(\tau)d\tau \geq 0 \quad \forall t \geq 0 \quad (1)$$

holds for admissible forces (f) and velocities (\dot{x}). Equation (1) states that the energy supplied to a passive network must be positive for all time [20], [21].

The elements of a typical haptic interface system include the virtual environment, the virtual coupling network, the haptic device controller, the haptic device, and the human operator. Many of the input and output variables of these elements of haptic interface systems can be measured by the computer and (1) can be computed in real time by appropriate software. This software is very simple in principle because at each time step, (1) can be evaluated with few mathematical operations.

The conjugate variables that define power flow in such a system are discrete-time values, and the analysis is confined to systems having a sampling rate substantially faster than the dynamics of the system. We assumed that there is no change in force and velocity during one sample time. Thus, we can easily “instrument” one or more blocks in

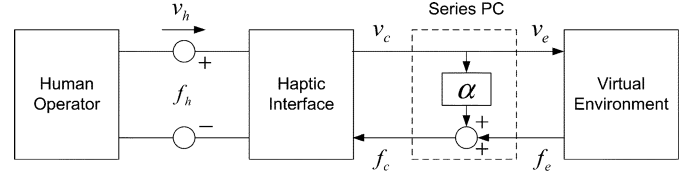


Fig. 2. Haptic interface system with series type PC for simulation.

the system with the following PO for a one-port network to check the passivity [see (1)]:

$$E_{\text{obsv}}(k) = \Delta T \sum_{j=0}^k f(t_j)v(t_j) \quad (2)$$

where ΔT is the sampling period, and $t_j = j \times \Delta T$. If $E_{\text{obsv}}(k) \geq 0$ for every k , this means the system does not generate energy. If there is an instance when $E_{\text{obsv}}(k) < 0$, this means the system generates energy and the amount of generated energy is $-E_{\text{obsv}}(k)$. Other research has allowed this constant force and velocity assumption to be relaxed [17], [19], and, in [17], the more accurate PO, which predict one-step ahead energy input, was proposed.

Consider a one-port system which may be active. Depending on operating conditions and the specifics of the one-port element’s dynamics, the PO may or may not be negative at a particular time. However, if it is negative at any time, we know that the one-port may then be contributing to instability. Moreover, since we know the exact amount of energy generated, we can design a time-varying element to dissipate only the required amount of energy. We call this element a PC. The PC takes the form of a dissipative element in a series or parallel configuration depending on the input causality [6].

Recently, reference energy following method was proposed [18] for removing sudden impulsive force of the PC with the following time-varying energy threshold instead of fixed zero energy threshold as follows:

$$W(k) = \sum_{j=0}^k f(t_{j-1})(x(t_j) - x(t_{j-1})) \geq E_{\text{ref}}(t_k) \quad \forall t_k \geq 0 \quad (3)$$

where $W(k)$ is the PO value for the case of impedance causality, which is the net energy input to a one-port network from 0 to t_k , and $E_{\text{ref}}(t_k)$ is the time-varying reference energy threshold which can be designed using VE model information or conjugate pair of input/output signal.

Please refer to [6], [16]–[18] for more detail about time domain passivity control approach.

III. ANALYSIS OF THE NOISY BEHAVIOR OF THE PO/PC

In this section, the main reasons of the noisy behavior are investigated through the simulation of a one-DOF haptic interface system (Fig. 2), consists of the human operator (HO), the haptic interface (HI), the PC, and the VE with impedance causality. Electrical circuit representation is used between HO and HI since the causality is hard to be defined at this kind of physical interaction port, and input-output representation is used between HI and VE because this is a use—defined signal port. There were well know researches about human dynamics in man/machine systems [12], [13]. However, in this paper, human and device are assumed to be one-DOF linear time invariant models as used in many other researches [1], [5], [6] for making the problem as simple as possible. The following simulation parameters were used for HO and HI:

$$\begin{aligned} M_{\text{HO}} &= 0.1 \text{ (kg)}, & B_{\text{HO}} &= 0.5 \text{ (N} \cdot \text{s/m)}, & K_{\text{HO}} &= 50 \text{ (N/m)}, \\ M_{\text{HI}} &= 0.2 \text{ (kg)}, & B_{\text{HI}} &= 0.0 \text{ (N} \cdot \text{s/m)}, & K_{\text{HI}} &= 0.0 \text{ (N/m)}. \end{aligned}$$

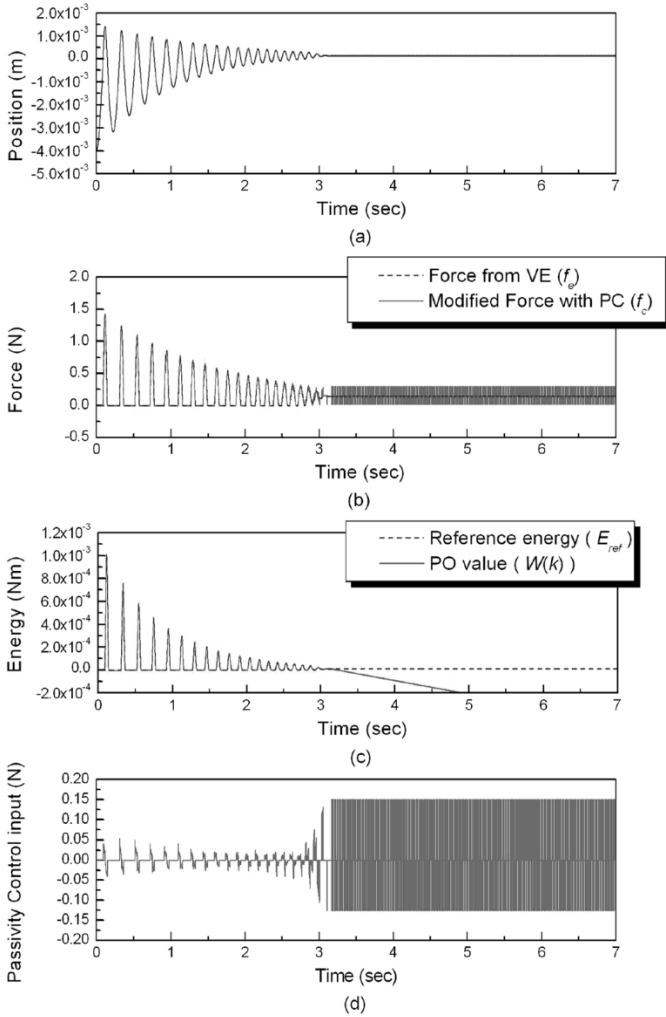


Fig. 3. Contact response with the energy following PO/PC [18] for the high stiffness VE ($K = 1000$ N/m). PC was noisy during the period of low velocity.

Note that the HI and HO have very low damping, and the high stiffness VE consists of a first order, penalty based spring model ($K = 1000$ N/m) executed at 1000 Hz. Two separate simulations with 1.0×10^5 Hz, one in Matlab/simulink, and one in a C program using trapezoidal integration were used including sensor quantization effect (minimum resolution is 1.0×10^{-5} (m)). The most recent PO/PC approach, which makes the energy input follows the desired reference energy behavior [18] was used at 1000 Hz.

The HI was pushed to make a contact with the high stiffness VE at Position ≥ 0 . The contact seemed stable [Fig. 3(a)] on the position response, but the PC input was chattering [Fig. 3(d)] and the PO value kept falling down to more negative value [Fig. 3(c)] during the period of low velocity. As a result, operator felt small and continuous vibration. Note that we bounded the PC force to escape the sudden big force change.

Fig. 4 shows the one-step backward velocity ($v(k) = (x(t_k) - x(t_{k-1})) / (\Delta T)$) of the above simulation. One-step backward velocity is the most appropriate velocity notation for explaining the effect of the velocity to the PO value (3). When the velocity was converged to the minimum resolutions ($\pm 1.0 \times 10^{-2}$ m/s), it started chattering with high frequency.

There are two undesirable behaviors of the velocity which make the PO/PC ineffective due to the limited resolution of the position sensor.

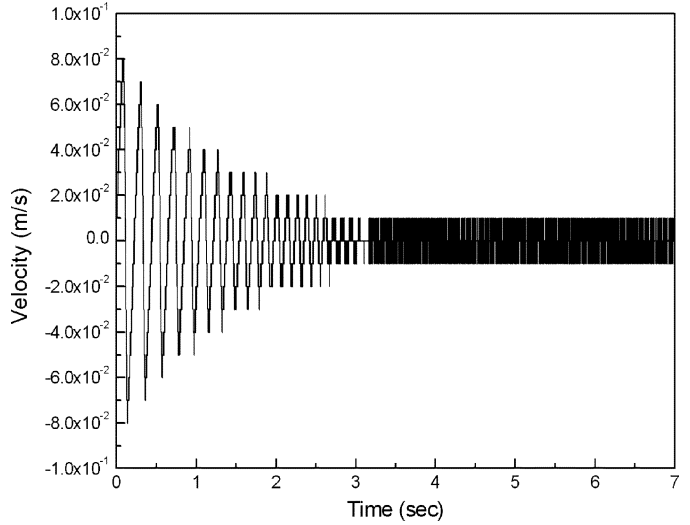


Fig. 4. Numerical backward velocity during the interaction. Velocity was chattering between minimum resolutions when $t_k > 2.5$ s.

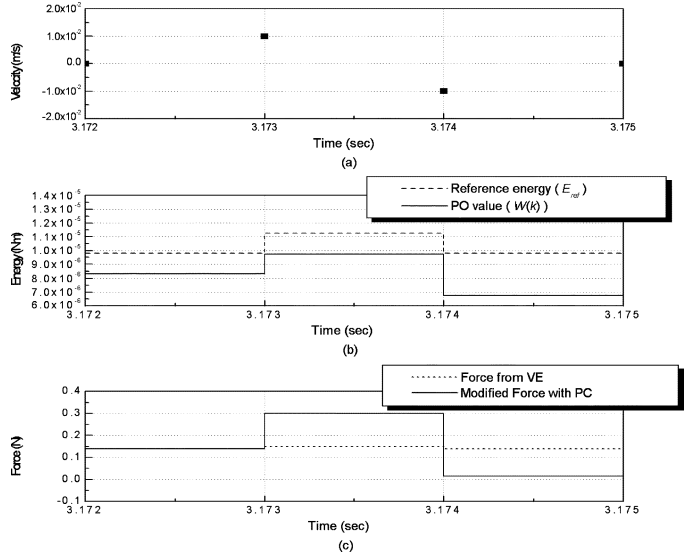


Fig. 5. Sudden sign change of the velocity and its effect to the PO value.

A. Sudden Sign Change of the Velocity

When the sign of the numerical velocity is suddenly changed from positive (or negative) at step k to negative (or positive) at step $k + 1$, the energy difference between the PO value and the reference energy is increased even with the PC force. Fig. 5 shows the magnified velocity and energy behavior of the above simulation. When the sign of the velocity was positive at $t = 3.173$ (s) [Fig. 5(a)], the PC increased the output force (Fig. 5(c)) to reduce the energy difference [Fig. 5(b)]. However the energy difference was increased when the velocity became negative at $t = 3.174$ (s) since the PO update rule is like

$$W(k + 1) = W(k) + f_c(k)v(k + 1)\Delta T. \quad (4)$$

This undesirable behavior can be explained with position versus force response of a VE as well. Before we explain the main idea, it is worth while to remind the example in our previous paper [17]. We have shown position versus force response of a VE which composed of a linear spring (Fig. 6). It has shown a staircase shape due to the discrete-time sampling, the limited resolution of the position sensor and the ZOH. The solid line indicates the behavior of the ideal linear

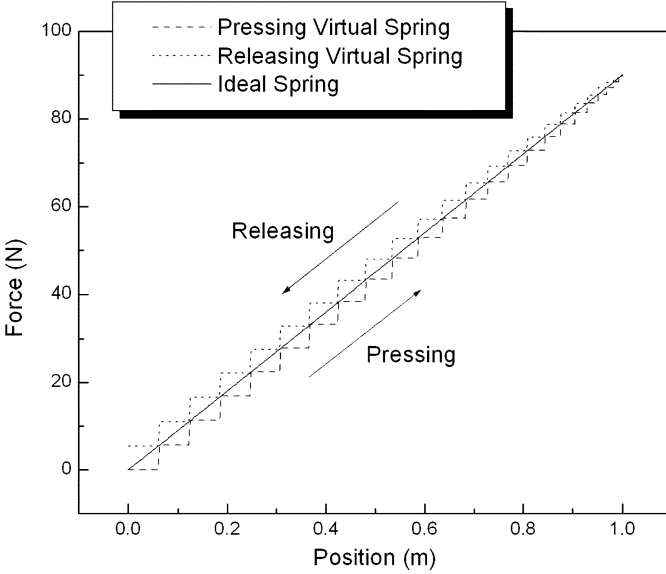


Fig. 6. Position versus force response of a virtual spring.

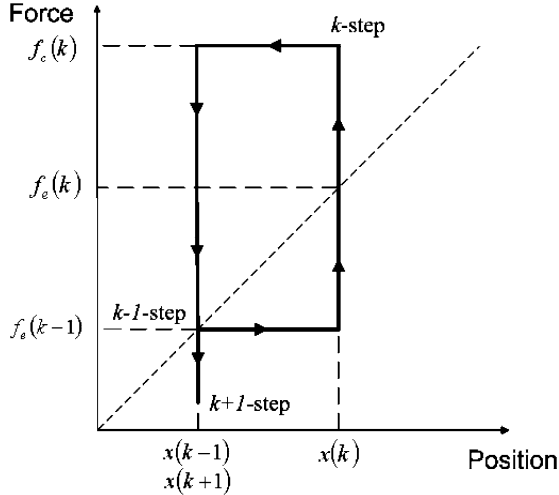


Fig. 7. Position versus force response when the velocity sign is changed in one sample time.

spring. The dashed line shows the case when the VE is pressed, and the dotted line shows the case when the VE is released. The area below each curve is the amount of energy that is dissipated and produced during the pressing and releasing process, respectively. The VE dissipates less energy, and produces more energy compared to the ideal spring. Thus, the VE is active while the ideal spring is passive. In [18], the PC was activated to shift up the dashed line and shift down the dotted line for making the net energy of the VE following the energy behavior of the ideal spring.

The measured position versus force response with PC is magnified for the case when the sign of the velocity is changed in one sample time (Fig. 7). Assume that the measured position was increased from $x(k-1)$ to $x(k)$ at step k , and back to the initial value at step $k+1$. If both the PO and the reference energy had the same value ($E(k-1)$) at step $k-1$, each values at step k would be as follows:

$$\begin{aligned} W(k) &= E(k-1) + f_e(k-1)(x(k) - x(k-1)) \\ E_{\text{ref}}(k) &= E(k-1) + f_e(k-1)(x(k) - x(k-1)) \\ &\quad + \frac{1}{2}(f_e(k) - f_e(k-1))(x(k) - x(k-1)) \end{aligned}$$

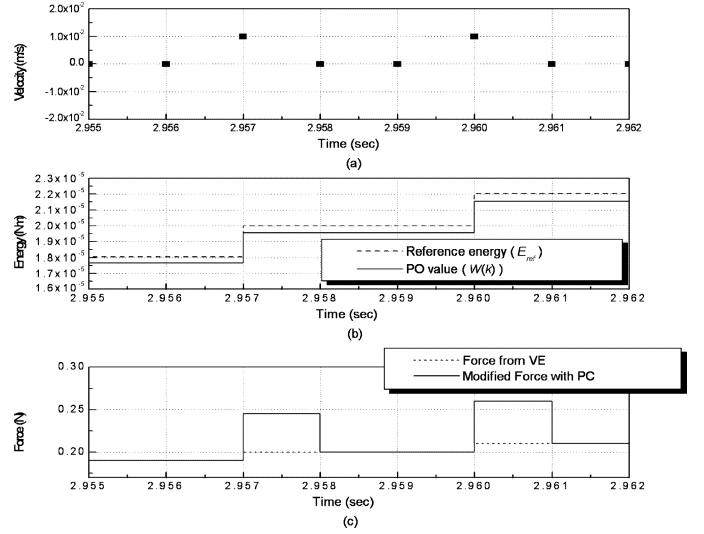


Fig. 8. Zero velocity after the PC action and its effect to the PO value.

where the amount of increment is the area below each curve. Since the PO value was less than the reference energy, the PC was activated to make the PO value follows the reference energy based on the current positive velocity. As a result, the force output was increased from $f_e(k)$ to $f_c(k) (= f_e(k) + f_{PC}(k))$, where $f_{PC}(k)$ is the passivity control input. However, the energy difference between the PO value and the reference energy was even increased at step $k+1$ since the sign of the velocity was suddenly changed.

$$\begin{aligned} W(k+1) &= E(k-1) + f_e(k-1)(x(k) - x(k-1)) \\ &\quad + f_c(k)(x(k+1) - x(k)) \\ &= E(k-1) + (f_e(k-1) - f_c(k))(x(k) - x(k-1)) \\ E_{\text{ref}}(k+1) &= E(k-1) + f_e(k-1)(x(k) - x(k-1)) \\ &\quad + \frac{1}{2}(f_e(k) - f_e(k-1))(x(k) - x(k-1)) \\ &\quad + f_e(k-1)(x(k+1) - x(k)) \\ &\quad + \frac{1}{2}(f_e(k) - f_e(k-1))(x(k+1) - x(k)) \\ &= E(k-1). \end{aligned}$$

With this velocity change, certain amount of energy ($(f_c(k) - f_e(k-1))(x(k) - x(k-1))$) was produced while the reference energy got back to the initial value. If the same situation happens several times, the energy difference become bigger, and the magnitude of the PC input will be increased.

B. Zero Values of the Velocity

Even though the sudden sign change of the velocity increased the energy difference between the PO value and the reference energy, the PC is supposed to make up for the energy difference for the rest of the cases. However, the PC could not give any effect for compensating the energy difference during the period of low velocity since the numerically calculated velocity were zero for the most of the time due to the resolution of the position sensor.

Fig. 8 shows the case by magnifying the above simulation result (Fig. 3). Even though the PC was activated at $t = 2.957$ (s) (Fig. 8(c)) and increased the output force, the energy difference at the next step ($t = 2.958$ (s)) was not changed [Fig. 8(b)] due to the zero velocity at $t = 2.958$ (s) [Fig. 8(a)].

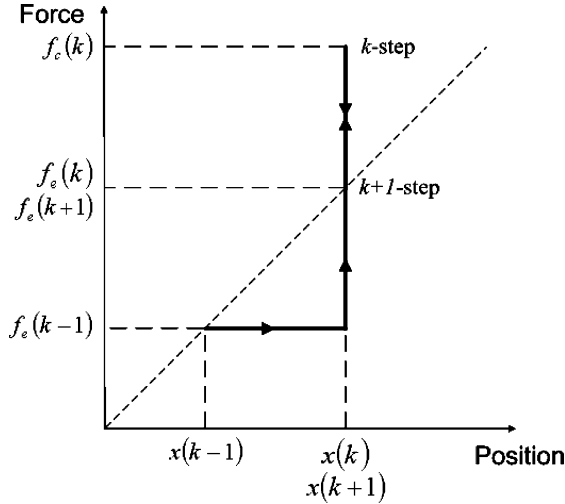


Fig. 9. Position versus force response when the velocity become zero after the PC action.

Assume that the velocity at step k was positive, and zero at step $k+1$ (Fig. 9). The PO values at step k and $k+1$ would be

$$\begin{aligned} W(k) &= E(k-1) + f_c(k-1)(x(k) - x(k-1)) \\ W(k+1) &= E(k-1) + f_c(k-1)(x(k) - x(k-1)) \\ &\quad + f_c(k)(x(k+1) - x(k)) \\ &= E(k-1) + f_c(k-1)(x(k) - x(k-1)). \end{aligned}$$

Even though the PC was activated at step k to make the PO follow the reference energy, the PC could not give any effect to the PO value at step $k+1$ since there was no position displacement ($x_k = x_{k+1}$). Therefore, the PC even makes the performance feel worse without any energy modification.

IV. METHODS FOR REMOVING THE NOISY BEHAVIOR

Through deep analysis, we found two main reasons of the noisy behavior during the period of the low velocity. The first one was the sudden sign change of the numerically calculated velocity in one sample time, and the second one was the zero value of the velocity after the PC action. In this section, methods to remove the noisy behavior are proposed based on the above analysis.

The first idea we could apply for solving this noisy behavior is estimating the velocity. A starting point of the velocity/displacement estimation was in [9]. Relatively nonconservative velocity filter in [7] was used for the same simulation of Fig. 3. However, the results were much worse (Fig. 10). The estimation error from the delay of the filter made the PO value, based on the filtered velocity, greater than the reference energy. Therefore the PC was not activated even though the system was vibrating.

Following are two respective methods for removing undesirable behaviors which were introduced in Section III.

A. Ignoring the Produced Energy From the Velocity Sign Change

Fig. 11 shows the measured position and the actual position of the simulation (in Fig. 3) during the period of low velocity. In the simulation, quantization effect was considered as follows:

$$\begin{aligned} \text{If } x_1 - \Delta x \leq x(t_k) < x_1 \text{ then } x(k) &= x_1 - \Delta x \\ \text{else if } x_1 \leq x(t_k) < x_1 + \Delta x \text{ then } x(k) &= x_1 \end{aligned}$$

where Δx is the minimum resolution of the position sensor, and x_1 is an integer multiple of Δx . The actual position was varying while the

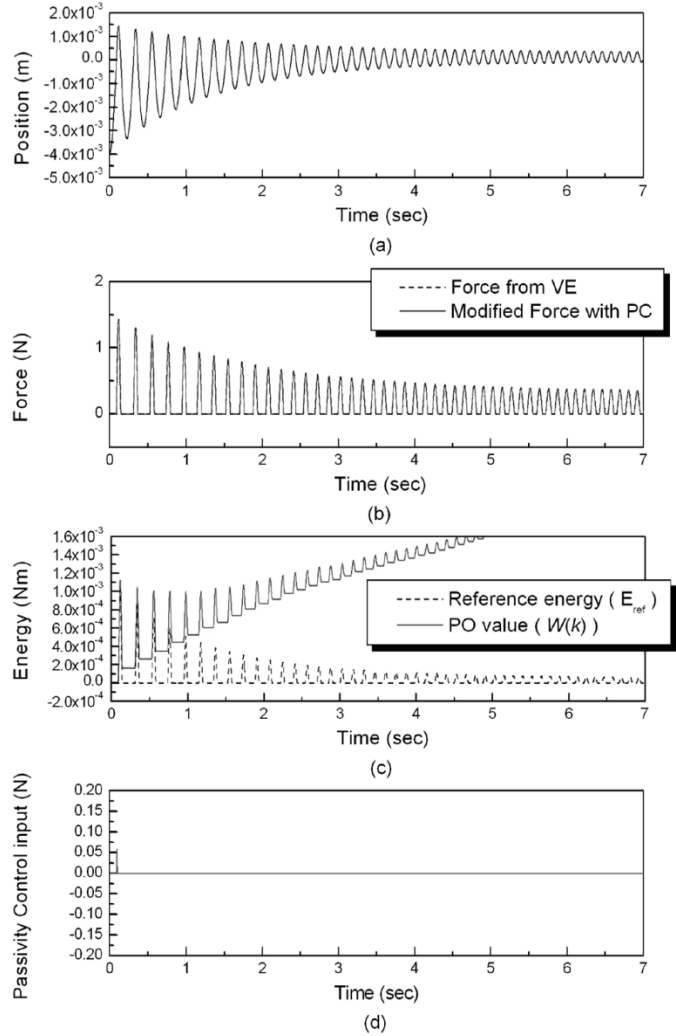


Fig. 10. Contact response with the energy following PO/PC, based on filtered velocity, for the high stiffness VE ($K = 1000$ N/m). The PO value was greater than the reference energy value even though the contact was unstable.

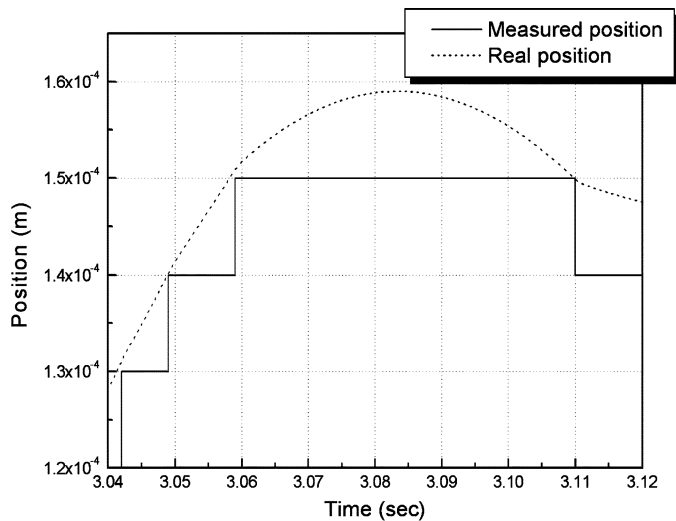


Fig. 11. Comparison of the actual position versus measured position during the period of low velocity. The actual position was varying while the measured position remained constant.

measured position was staying constant, and the small displacement near digitized line caused discrete change of the measured position. If

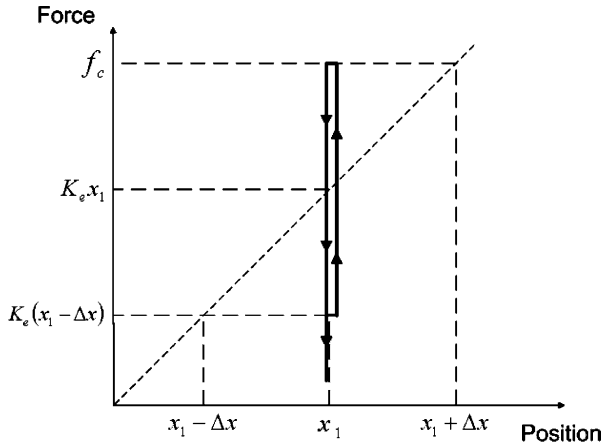


Fig. 12. Actual position versus force response when the sign of the velocity is suddenly changed in one sample time.

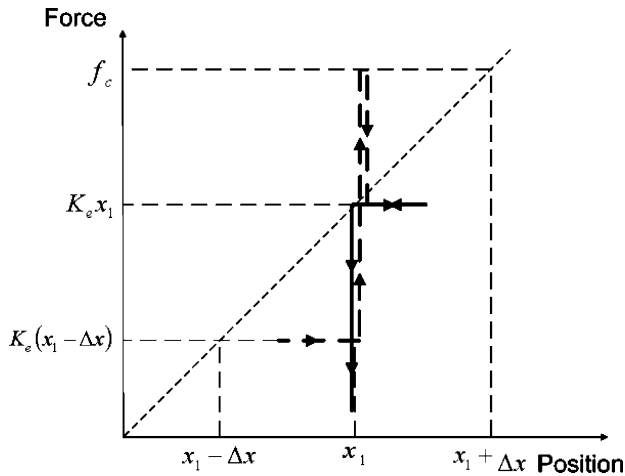


Fig. 13. Actual position versus force response when the sign of the velocity is changed during low velocity.

the actual position behavior is considered for the calculation of the PO, the more accurate and nonconservative PO value can be obtained for escaping the unnecessary PC operation.

Based on the observation in Fig. 11, the actual position versus force response is redrawn when the sign of the velocity is suddenly changed in one sample time (Fig. 12). Since we confined the analysis to systems that have fast enough sampling rate compared to the system mode, the width of the rectangle in Fig. 12 is closer to zero than it is to the rectangle in Fig. 7, so it is better to ignore it rather than include a rectangle like Fig. 7.

Not only a sudden sign change but also a slow sign change like Fig. 11 could give undesirable effect to the PO value. However this effect is ignorable if the sampling rate is fast enough. Fig. 13 shows different two paths of the actual position versus force response when it was compressed (dashed line) and released (solid line). Note that one sample time after the actual position crossed x_1 , the output force was decreased to $K_e x_1$ and stayed until the position became less than x_1 . This behavior produced two rectangles. The area of upper one is the dissipated energy with the PC, and the lower one is the produced energy due to the velocity sign change. If the PO value and the reference energy were same at the beginning of this graph, f_c would be same as $K_e(x_1 + \Delta x)$. Please see [18]. Therefore the dissipated and produced

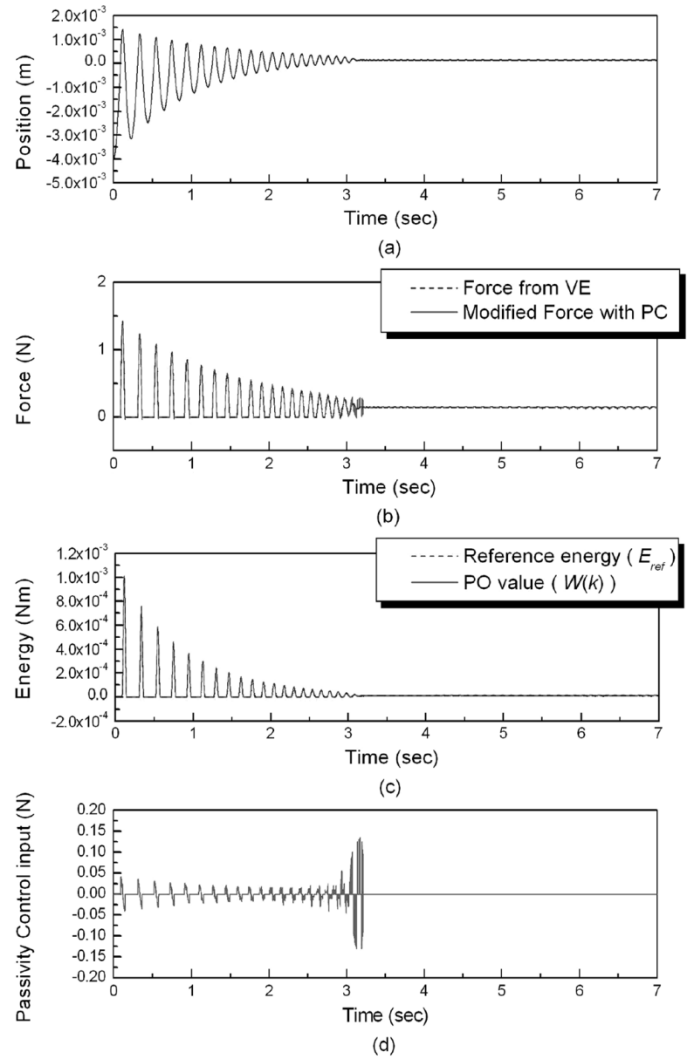


Fig. 14. Contact response with the proposed energy ignoring method from sign change.

energy would be summed to almost zero as long as the actual position is not suddenly changed.

We assume that the inherent dissipative elements in HI and HO are enough to dissipate the produced energy for the above two cases, if there is. As a result, it can be ignorable that the negative effect of the PO value from the above two sign changes.

Fig. 14 shows the result of the simulation which ignores the change of the PO value from the sign change. Noisy behavior and the PC control force were significantly reduced. However, during the transient time (near $t = 3$ (sec)), some levels of noisy behavior remained [Fig. 14(b), (d)]. This was because the zero value of the velocity could not contribute to modify the PO value.

B. Holding the PC Force During Zero Velocity

Since we found that the actual velocity was nonzero, even though the numerically calculated velocity was zero, The PC force was held during the zero velocity for using actual velocity information. In Fig. 15, the PC force was held during the measured position was constant. Even though the measured position was constant, the actual position was gradually increased from x_1 to $x_1 + \Delta x$. Therefore, the PC force could contribute to compensate the energy difference. Moreover, once the measured position became greater than or equal to $x_1 + \Delta x$, the

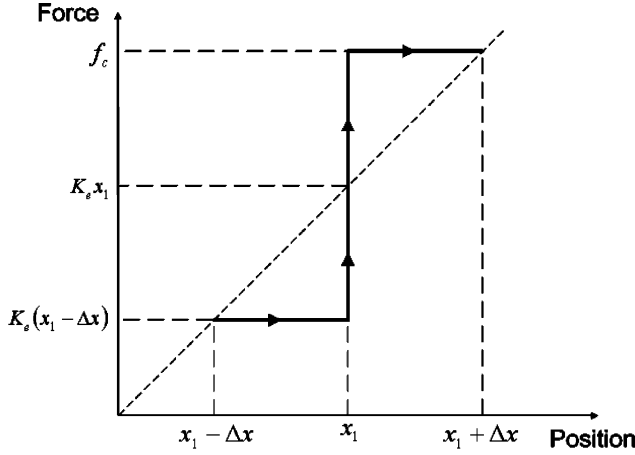


Fig. 15. Actual position versus force response when the PC force is held while the velocity is zero.

TABLE I
IMPROVED PO/PC ALGORITHM FOR REMOVING THE NOISY BEHAVIOR

```

If  $|\Delta x(k)| < \delta$  {
     $f_{PC}(k) = f_{PC}(k-1)$ 
     $W(k) = W(k-1) + f_c(k-1)\Delta x(k)$ 
} else {
    If  $(\Delta x(k) = -Prev_{\Delta x}) \& (|\Delta x(k)| = \delta)$  {
         $W(k) = W(k-1) - Prev_{f_c} Prev_{\Delta x}$ 
    } else {
         $W(k) = W(k-1) + f_c(k-1)\Delta x(k)$ 
    }
     $Prev_{\Delta x} = \Delta x(k)$ 
     $Prev_{f_c} = f_c(k)$ 
    If  $(W(k) < E_{ref}(k))$  {
         $f_{PC}(k) = -\frac{W(k) - E_{ref}(k)}{\Delta x(k)}$ 
    } else {
         $f_{PC}(k) = 0$ 
    }
}
 $f_c(k) = f_c(k) + f_{PC}(k)$ 
    
```

compensated energy was automatically updated considering the actual position displacement without any PO modification.

Table I summarizes the mentioned overall compensation algorithm of the PO/PC including ignoring the produced energy and holding the PC force schemes, where δ is the minimum resolution of the position sensor, $\Delta x(k) = x(k) - x(k-1)$, and f_{PC} is the PC force.

The proposed holding and ignoring algorithm were implemented to the same simulation as Fig. 14. The noisy behavior during the transient state was removed [Fig. 16(b)], and the unnecessary PC force was also significantly reduced [Fig. 16(d)].

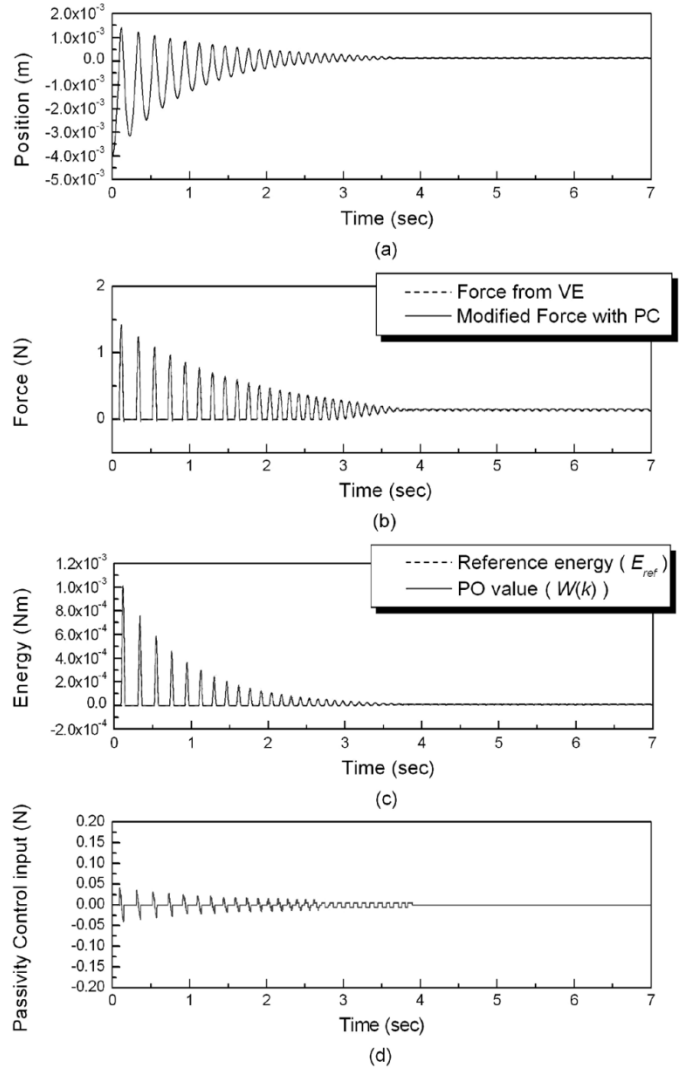


Fig. 16. Contact response with the PC force holding and the energy ignoring method as well.

V. EXPERIMENTAL RESULTS

The similar experiment with the simulation in Sections III and IV was done with a PHANTOM haptic device. We made a contact with a VE ($K = 1000$ N/m) at Position > 0 by applying the previous PO/PC in [18]. The device was pushed to make a contact and operator kept pushing the VE to maintain the contact. Without the proposed methods, the similar result with the simulation (Fig. 3) was obtained. The position response seemed stable [Fig. 17(a)], but the modified force was vibrating [Fig. 17(b)], and operator felt small and continuous vibration during the period of low velocity (see Fig. 17).

If the experimental result was magnified, similar trends of the velocity and the PO responses were found, which were the main reasons of the noisy behavior as we found in Figs. 5 and 8 through the simulation. During $t = 1.556-1.561$ (sec), the sudden and continuous sign changes of the velocity and its negative effect to the PO value were found [Fig. 18(a)–(c)] like in Fig. 5. Fig. 19(a)–(c) shows the zero values of the velocity after PC action and its effect to the PO value. During $t = 1.543-1.548$ (s) the same behavior as in Fig. 8 was found. Therefore, it is reasonable to apply the proposed methods from the simulation to the experiment for compensating the noisy behavior.

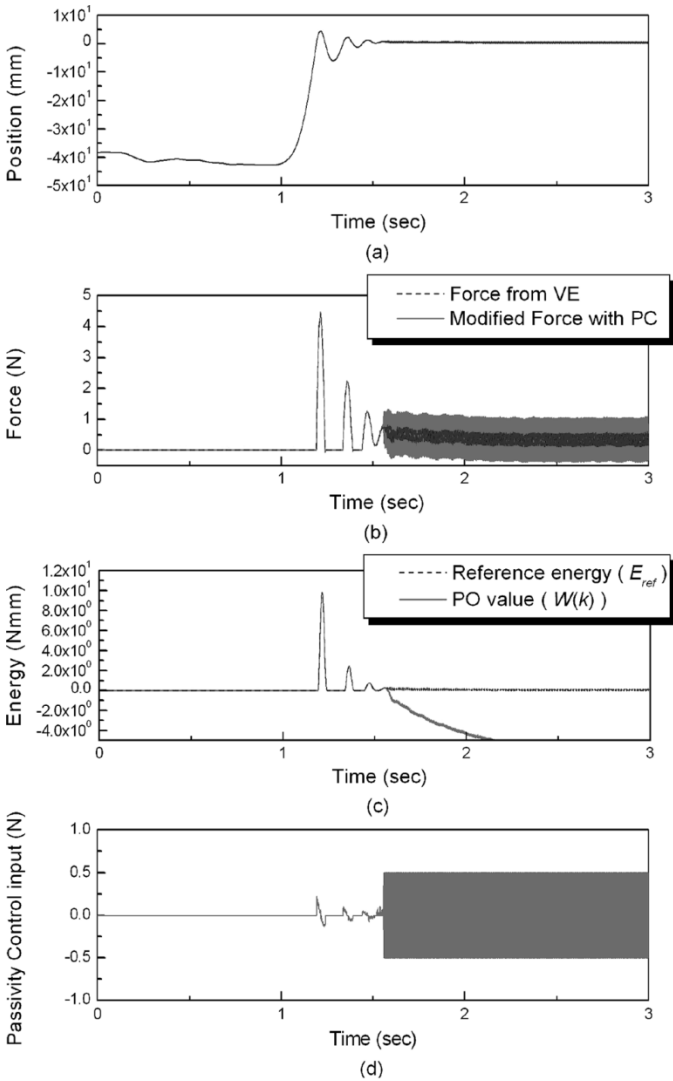


Fig. 17. Experimental result with the PO/PC without the proposed methods.

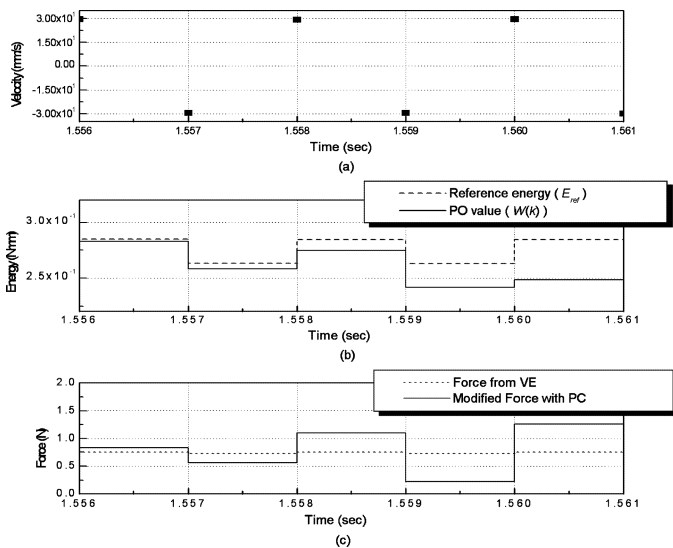


Fig. 18. Sudden sign change of the velocity and its effect to the PO value. Experimental results are similar to the simulation results in Fig. 5.

By applying the proposed methods, the noisy behavior was significantly removed, and operator felt smooth force as shown in Fig. 20.

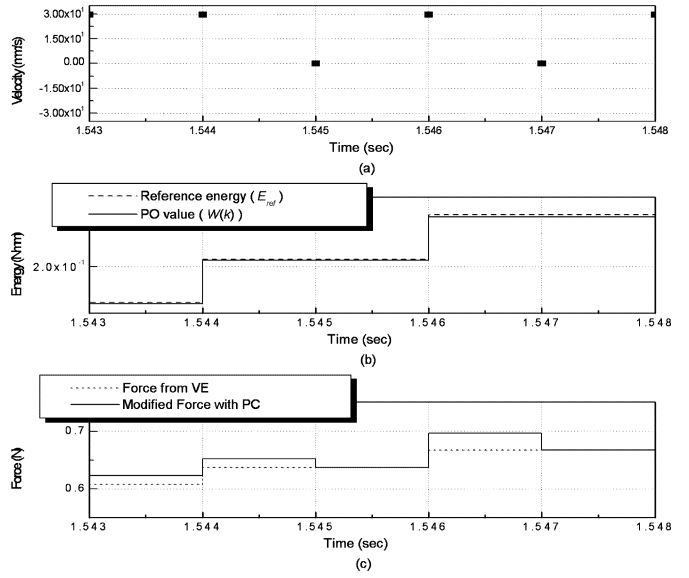


Fig. 19. Zero velocity after the PC action and its effect to the PO value. Experimental results are similar to the simulation results in Fig. 8.

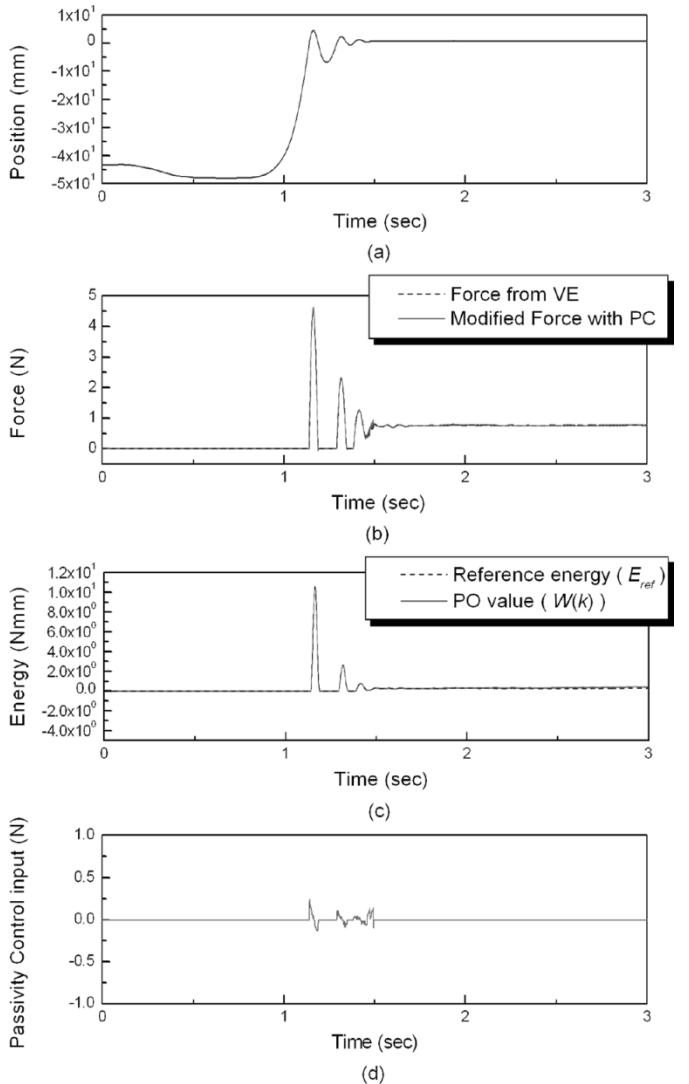


Fig. 20. Experimental result with the PO/PC with the proposed methods.

VI. CONCLUSION AND FUTURE WORKS

In this paper, methods to remove the noisy behavior of the PO/PC are proposed through the deep analysis of the simulation and experiment. There were two main reasons of the noisy behavior. One of them was the sign change of the numerically calculated velocity. This was because we can not help estimating the future velocity for calculating the current PO/PC. The other one was the zero value of the velocity after the PC action. Since the calculated velocity was zero for the most of the time during the period of low velocity even though the actual velocity was not, the PO became conservative and generated the non-necessary PC force. The method for solving the first problem was ignoring the difference of the PO value from the velocity sign change based on the assumption that the actual energy difference is significantly small and can be dissipatable with the inherent damping of HO and HI. The other method for solving the second problem was holding the PC force during zero velocity since the actual velocity is not zero. The feasibility of the proposed methods was proved through the simulation and the experiment, and the PO/PC approach became more practical with the proposed methods.

In some case, the produced energy from the velocity sign change may not be ignorable. If the sampling rate is not fast enough compared to the system mode, the position sensor can not catch the exact instance when the actual position crosses the digitized line. As a result, the width of the rectangle in Fig. 12 will be increased, and the amount of the produced energy may become greater than the allowable energy. Therefore, it is better to turn off the PC when the velocity sign change is repeated. To find the exact condition when the PO/PC is not effective anymore, we are studying the limitation of the PO/PC approach as a further work.

REFERENCES

- [1] R. J. Adams and B. Hannaford, "Stable haptic interaction with virtual environments," *IEEE Trans. Robot. Automat.*, vol. 15, no. 3, pp. 465–474, Jun. 1999.
- [2] R. J. Anderson and M. W. Spong, "Asymptotic stability for force reflecting teleoperators with time delay," *Int. J. Robot. Res.*, vol. 11, no. 2, pp. 135–149, 1992.
- [3] F. Barbagli, D. Prattichizzo, and K. Salisbury, "Multirate analysis of haptic interaction stability with deformable objects," in *IEEE Int. Conf. Decision Control*, Italy, 2002, pp. 917–922.
- [4] J. E. Colgate and J. M. Brown, "Factors affecting the Z-width of a haptic display," in *Proc. IEEE Int. Conf. Robot. Automat.*, San Diego, CA, May 1994, pp. 3205–3210.
- [5] J. E. Colgate and G. Schenkel, "Passivity of a class of sampled data systems: Application to haptic interfaces," in *Proc. American Control Conf.*, Baltimore, MD, 1994, pp. 3236–3240.
- [6] B. Hannaford and J. H. Ryu, "Time domain passivity control of haptic interfaces," *IEEE Trans. Robot. Autom.*, vol. 18, no. 1, pp. 1–10, Feb. 2002.
- [7] F. Janabi-Sharifi, V. Hayward, and C.-S. J. Chen, "Discrete-time adaptive windowing for velocity estimation," *IEEE Trans. Contr. Syst. Technol.*, vol. 8, no. 6, pp. 1003–1009, Dec. 2000.
- [8] Y. S. Kim and B. Hannaford, "Some practical issues in time domain passivity control of haptic interfaces," in *Proc. IEEE/RSJ Int. Conf. Intelligent Robotics Systems*, Maui, HI, 2001, pp. 1744–1750.
- [9] B. Kumar and S. C. Dutta Roy, "Design of digital differentiators for low frequencies," *Proc. IEEE*, vol. 76, pp. 287–289, Mar. 1988.
- [10] D. Lee and P. Y. Li, "Toward robust passivity: A passive control implementation structure for mechanical teleoperators," in *Proc. 11th Haptics Teleoperator Symp.*, Los Angeles, CA, Mar. 2003, pp. 132–139.
- [11] S. Mahapatra and M. Zefran, "Stable haptic interaction with switched virtual environments," in *Proc. IEEE Int. Conf. Robot. Automat.*, Taipei, Taiwan, 2003, pp. 14–19.
- [12] D. T. McRuer, "Human dynamics in man-machine systems," *Automatica*, vol. 16, no. 3, pp. 237–253, 1980.
- [13] D. T. McRuer and E. S. Krendel, "The human operator as a servo element," *J. Franklin Inst.*, vol. 267, pp. 381–403, 1959.

- [14] B. E. Miller, J. E. Colgate, and R. A. Freeman, "Environment delay in haptic systems," in *Proc. IEEE Int. Conf. Robotics Automation*, San Francisco, CA, Apr. 2000, pp. 2434–2439.
- [15] G. Niemeyer and J. J. Slotine, "Stable adaptive teleoperation," *IEEE J. Ocean. Eng.*, vol. 16, no. 2, pp. 152–162, Feb. 1991.
- [16] J. H. Ryu, D. S. Kwon, and B. Hannaford, "Stable teleoperation with time domain passivity control," *IEEE Trans. Robot. Autom.*, vol. 20, no. 2, pp. 365–373, Apr. 2004.
- [17] J. H. Ryu, Y. S. Kim, and B. Hannaford, "Sampled and continuous time passivity and stability of virtual environments," *IEEE Trans. Robot.*, vol. 20, no. Aug., pp. 772–776, 2004.
- [18] J. H. Ryu, B. Hannaford, C. Preusche, and G. Hirzinger, "Time domain passivity control with reference energy behavior," in *Proc. IEEE/RSJ Int. Conf. Intelligent Robotics Systems*, Las Vegas, NV, 2003, pp. 2932–2937.
- [19] S. Stramigioli, C. Secchi, and A. J. van der Schaft, "A novel theory for sampled data system passivity," in *IEEE/RSJ Int. Conf. Intelligent Robotics Systems*, Switzerland, 2002, pp. 1936–1941.
- [20] A. J. van der Schaft, *L₂-Gain and Passivity Techniques in Nonlinear Control*, ser. Communications and Control Engineering Series. Berlin, Germany: Springer-Verlag, 2000.
- [21] J. C. Willems, "Dissipative dynamical systems—Part I: General theory," *Arch. Rat. Mech. An.*, vol. 45, pp. 321–351, 1972.
- [22] C. B. Zilles and J. K. Salisbury, "A constraint-based god-object method for haptic display," in *Proc. IEEE/RSJ Int. Conf. Intelligent Robot. Systems*, Pittsburgh, PA, 1995, pp. 146–151.

Inverse Jacobian Regulator With Gravity Compensation: Stability and Experiment

C. C. Cheah and H. C. Liaw

Abstract—Task-space regulation of robot manipulators can be classified into two fundamental approaches, namely, transpose Jacobian regulation and inverse Jacobian regulation. In this paper, two inverse Jacobian regulators with gravity compensations are presented, and the stability problems are formulated and solved. It is shown that the inverse Jacobian systems can be stabilized, and there exists a region of attraction such that the system remains stable. Our results show that the two fundamental approaches are two dual controllers, in the sense that the transpose Jacobian matrix can be replaced by the inverse Jacobian matrix and vice versa. The theoretical results are verified experimentally by implementing the inverse Jacobian regulators on an industrial robot, PUMA560.

Index Terms—Inverse Jacobian, regulation, robot control, stability.

I. INTRODUCTION

Robot control tasks are typically specified in task space such as visual space or Cartesian space. Therefore, if the robot controllers are formulated in joint space [1]–[9], it is required to solve the inverse kinematics problem to derive a desired joint configuration for the robot. To eliminate the problem of solving the inverse kinematics, the concept of task-space control [1], [10]–[14] for robot manipulators is proposed. The basic idea of the task-space control is to formulate a control scheme

Manuscript received January 6, 2004. This paper was recommended for publication by Associate Editor Y. Liu and Editor H. Arai upon evaluation of the reviewer's comments. This paper was presented in part at the IEEE International Conference on Control Applications, Taiwan, R.O.C., 2004.

C. C. Cheah is with School of Electrical and Electronic Engineering, Nanyang Technological University, 639798 Singapore (e-mail: ECCCheah@ntu.edu.sg). H. C. Liaw is with Mechatronics Group, Singapore Institute of Manufacturing Technology, 638075 Singapore.

Digital Object Identifier 10.1109/TRO.2005.844674